# An allgorithm for mesh rezoning with application to strain localization problems

Please check the document version of this publication:

• A submitted manuscript is the version of the article upon submission and before peer-review. There can be important differences between the submitted version and the official published version of record. People interested in the research are advised to contact the author for the final version of the publication, or visit the DOI to the publisher's website.
• The final author version and the galley proof are versions of the publication after peer review.
• The final published version features the final layout of the paper including the volume, issue and page numbers.

Link to publication

# AN ALGORITHM FOR MESH REZONING WITH APPLICATION TO STRAIN LOCALIZATION PROBLEMS

**M. A. Gutiérrez, R. de Borst, J. C. J. Schellekens** and **L. J. Sluys**

Delft University of Technology, Department of Civil Engineering, P.O. Box 5048, 2600 GA Delft,
The Netherlands

**Abstract**—This paper describes an algorithm for automatic rezoning of the finite element mesh, which can be used in adaptivity techniques where the initial topology is conserved. Difficulties like the definition of an adequate mesh density, its continued interpolation and the description of curved boundaries have been overcome successfully. The algorithm has been used in some strain localization problems. The output of a first analysis with a coarse, constant density mesh is used as an indicator to control the mesh spacing in a subsequent calculation, leading to an improved solution. The improvement of the solution upon remeshing is shown.

## 1. INTRODUCTION

The phenomenon of strain localization in softening materials can be described as the presence of a thin zone where the plastic strain accumulates progressively, while the rest of the structure unloads. Not all the possible descriptions for a continuum can be used to simulate a localization phenomenon. The use of a classical continuum description leads to a mathematically ill-posed boundary value problem, which has the consequence that the results are entirely dependent on the finite element mesh spacing. A higher-order or rate dependent method must be used in order that the solution converges to a unique, physically meaningful value upon mesh refinement. An overview of most of these approaches has been given by Sluys [1].

The finite element simulation of localization problems requires a large number of degrees of freedom to describe the phenomenon properly. This number should be large in the localization zone, but can be lower in the rest of the structure. If the position and characteristics of the localization zone are not known *a priori*, the analysis needs a number of elements that can be prohibitively large for practical computations.

The difficulty can be overcome by adaptive meshing techniques. The aim is to provide an element density in the mesh that is locally adjusted to the degree of non-linearity. A preliminary analysis is performed with a coarse mesh; the mesh is refined where needed and the analysis is repeated with the new, improved mesh.

Most of the adaptive meshing techniques create a completely new mesh, but in some formulations the mesh topology (i.e. the adjacency relationship of the elements) is conserved. An example is the so-called Arbitrary Lagrangian–Eulerian [2]–[4], where the mesh motion is independent of the material displacements. The method was primarily developed for the analysis of geometrical non-linearities and fluid-structure interaction problems. In this article, we shall refer to remeshing techniques as rezoning algorithms.

This paper is organized as follows: firstly, a concise review of the requirements imposed upon remeshing algorithms is given; on the basis of this, an algorithm for mesh refinement is developed. Finally, the developed algorithm is used in a mesh adaptivity analysis of a biaxial shear-band test.

## 2. BACKGROUND

The developed remeshing algorithm belongs to the class of rezoning methods, in which the nodal positions are modified to accommodate the desired mesh density at prescribed locations, while the global mesh topology (i.e. the adjacency relationship of the elements) is conserved. Rezoning techniques consist of defining a weight function at each point of the mesh and executing an algorithm such that the mesh is adapted in a fashion that the elements are small where the weight function has a high value and large where it has a low value. They usually result in an iterative procedure. Some important points in rezoning algorithms are:

- The weight function is dependent on the spatial position. This means that its value must be updated after every iteration is completed.
- The weight function is rarely available in a closed form, because it usually derives from a previous analysis. Consequently, it must be evaluated via interpolation with the shape functions.

- The resulting element size must be inversely proportional to the given weight function. This means that if the weight function has a value five in point $P$ and a value one in point $Q$, the element $P$ must be five times smaller than that in $Q$.
- The shape of the resulting elements must be not too distorted, in order to assure the reliability of the analysis. This is of special importance when quadrilateral elements are used.
- The remeshing algorithm should impose no limitations on the shape and topology of the discretized domain.

Typically, rezoning is performed by solving an elliptical equation by means of the Finite Difference Method, using forcing functions dependent on the weight function [5], [6], or by directly imposing the rezoning principle mentioned above, that is, the weight function times the element size is constant throughout the mesh [5], [7]. These procedures usually result in long calculations and do not handle curved boundaries in a clear way. Another possible approach is the spring analogy [8], but in this case relative variations of the weight function are not well reflected in the resulting element size. As a result the requirement that the element size and the weight function should be inversely proportional is violated.

Giuliani [9] developed a remeshing algorithm for large boundary motion, as for instance occurs in boundary layers in fluids or in free surface flows. In this method the position of every node is adapted so as to minimize the average distortion of the elements to which it belongs. An iterative Gauß–Seidel procedure is used to determine the final nodal positions. The explicitness of this algorithm makes it possible to modify it such that mesh refinement is allowed without a significant increase of the computing time, if we relate the element distortion to the desired element size.

### 3. REZONING ALGORITHM

The developed rezoning algorithm is based on the technique described by Giuliani [9], as mentioned above, and is described in detail by Gutiérrez [10].

### 3.1. *Mesh density*

Let $\Omega$ be a domain discretized in finite elements. Consider a subdomain $\Delta\Omega$ containing $\Delta n$ elements. According to Cescotto and Wu [11], the mesh density at point $P$ can be defined as

$$\delta(P) = \lim_{\Delta\Omega \to 0} \frac{\Delta n}{\Delta\Omega}. \tag{1}$$

In this fashion, the total number of elements in $\Omega$ can be written as

$$n = \int_\Omega \delta \, d\Omega. \tag{2}$$

Equation (2) shows that $\delta$ cannot be chosen arbitrarily in cases where the mesh topology, and consequently the total number of elements, must be kept constant. Now suppose that function $w$ is used as density. Then, the total number of elements would be

$$m = \int_\Omega w \, d\Omega. \tag{3}$$

Without loss of generality, we can write

$$n = km, \tag{4}$$

where $k$ is a real constant, or equivalently

$$n = \int_\Omega kw \, d\Omega. \tag{5}$$

Comparison of expressions (2) and (5) shows how the mesh density can be obtained from the weight function. Among the possible choices the simplest solution is to require locally

$$\delta = kw. \tag{6}$$

From expression (5),

$$k = \frac{n}{\int_\Omega w \, d\Omega} \tag{7}$$

and consequently

$$\delta = \frac{nw}{\int_\Omega w \, d\Omega}. \tag{8}$$

### 3.2. *One-dimensional rezoning algorithm*

For line elements the rezoning algorithm is based on the definition of an elemental distortion in terms of element length, which is later globally minimized such that the resulting elements have a length as close as possible to the desired value.

3.2.1. *One-dimensional distortion metric.* The definition of a one-dimensional distortion metric is quite simple. It is taken as the square of the analogon of the strain that an $L$-length bar would experience if its actual length were $\hat{L}$,

$$D = \left(\frac{\hat{L} - L}{L}\right)^2. \tag{9}$$

The reason for the square is to avoid the sign effect and to provide function $D$ with $C^1$ continuity. Since the actual length of an element is

$$\hat{L} = x_2 - x_1, \tag{10}$$

where $x_1$ and $x_2$ are just its nodal coordinates, the distortion metric $D$ results in

$$D = \left(\frac{x_2 - x_1 - L}{\cdot L}\right)^2. \qquad (11)$$

### 3.2.2. Minimization of the local distortion.

The optimal values of $x_1$ and $x_2$ are those which make $D$ minimum,

$$\begin{cases} \dfrac{\partial D}{\partial x_1} = 0 \\[2mm] \dfrac{\partial D}{\partial x_2} = 0 \end{cases}, \qquad (12)$$

which, using eqn (11), is elaborated as

$$\begin{bmatrix} 1 & -1 \\ -1 & 1 \end{bmatrix} \begin{bmatrix} x_1 \\ x_2 \end{bmatrix} = \begin{bmatrix} -L \\ L \end{bmatrix}. \qquad (13)$$

System (13) is an elemental minimization of the distortion.

### 3.2.3. Minimization of the global distortion.

Next consider a one-dimensional domain

$$\Omega = \{x \in \mathbb{R} | x_0 \leqslant x \leqslant x_n\} \qquad (14)$$

discretized in $n$ line elements, $e_i$, which can be defined as

$$e_i = \{x \in \Omega | x_{i-1} \leqslant x \leqslant x_i\} \qquad (15)$$

where $x_j$, $j = 0-n$, are the nodal positions, and an optimal element length $L(x)$ is defined on every point of $\Omega$. System (13) can be written for every element, by evaluating the optimal length $L$ at its centre, in order to obtain a length $L_i$ for element $e_i$. After assembly, the global system is

$$\begin{bmatrix} 2 & -1 \\ -1 & 2 & -1 \\ & -1 & 2 & \cdot\cdot\cdot & & & 0 \\ & & \cdot\cdot & \cdot\cdot & \\ & & & & 2 & -1 \\ & & & & -1 & 2 & \cdot\cdot\cdot \\ & 0 & & & & \cdot\cdot & \cdot\cdot & -1 \\ & & & & & & -1 & 2 \end{bmatrix} \begin{bmatrix} x_1 \\ x_2 \\ x_3 \\ \vdots \\ \vdots \\ x_{i-1} \\ x_i \\ \vdots \\ x_{n-1} \end{bmatrix} = \begin{bmatrix} L_1 - L_2 + x_0 \\ L_2 - L_3 \\ L_3 - L_4 \\ \vdots \\ \vdots \\ L_{i-1} - L_i \\ L_i - L_{i+1} \\ \vdots \\ L_{n-1} - L_n + x_n \end{bmatrix}, \qquad (16)$$

where $x_0$ and $x_n$ have been kept fixed. Since $L_i$ is dependent on $x_{i-1}$ and $x_i$, eqn (16) is a non-linear system, which symbolically can be written as

$$\mathbf{A}\mathbf{x} = \mathbf{b}(\mathbf{x}). \qquad (17)$$

Since matrix $\mathbf{A}$ is constant, this system can be solved by a fixed-point iteration procedure, i.e.

$$\mathbf{x}^{k+1} = \mathbf{A}^{-1}\mathbf{b}(\mathbf{x}^k), \qquad (18)$$

where $k$ accounts for the iteration number.

After a first analysis and an estimation of the error, the desired (relative) mesh density is known. System (16) requires that the desired element length, $L$, is known in the whole $\Omega$. This can be computed from

$$L = \frac{1}{\delta} \qquad (19)$$

and $\delta$ is known from equation (8). The value of $L$ is finally interpolated by means of the shape functions.

### 3.3. Two-dimensional rezoning of a generic node

Consider the portion of a finite element mesh composed of quadrilaterals which is shown in Fig. 1. The polygon defined by the nodes connected to node $P_i$ via element sides is defined as the influence domain for node $P_i$ (shaded in Fig. 1). This influence domain is subdivided into triangles. The basic idea is to move node $P_i$ in order to minimize the average distortion of these triangles, measured in some sense, to be defined later.

The ideal triangle is taken as isosceles, with height $h^*$ and basis $\bar{b}$, where $h^*$ is the height it is expected to have and $\bar{b}$ is the average basis of all the triangles in the influence domain of node $P_i$. If $h$ represents the actual height of the triangle, and $d$ the distance between the projection of node $P_i$ on the basis of the triangle and its centrepoint $M$ (Fig. 2), the local distortion of a triangle can be written as

$$D = t\left(\frac{h - h^*}{h^*}\right)^2 + (1 - t)\left(\frac{2d}{\bar{b}}\right)^2. \qquad (20)$$

The first term of eqn (20) controls the triangle size and the second term determines its shape. Parameter $t$, $0 \leqslant t \leqslant 1$, controls the relative influence of each term. For $t \neq 1$ the mesh density will not exactly be as desired, because the second term introduces a certain "rigidization" and forces the elements to be as regular as possible. For $t = 1$ the second term is disregarded and the mesh density will be as close as possible to the desired density, but some elements can have a bad shape in zones of low density gradient. If values close to one are chosen, the resulting mesh should match the prescribed density properly and the element shape is optimal in zones of low density gradient.
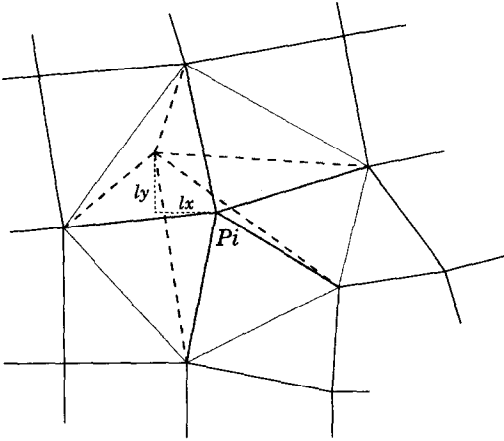
Fig. 1. Representation of the influence domain (shaded) of node $P_i$.

The distortion of the influence domain of node $P_i$ can simply be written as the sum of the individual distortion of the $\acute{n}$ triangles which constitute the influence domain, that is

$$\hat{D} = t \sum_{\acute{n}} \left(\frac{h - h^*}{h^*}\right)^2 + (1 - t) \sum_{\acute{n}} \left(\frac{2d}{\bar{b}}\right)^2. \qquad (21)$$

Let $l_x$ and $l_y$ be the components of the translation of node $P_i$ required to achieve its rezoning. Consider the generic triangle shown in Fig. 2. After rezoning the triangle area, $a$, and the basis, $b$, are given by [9]

$$a = \tfrac{1}{2}(pl_x + ql_y) + a' \qquad (22)$$

and

$$b = \sqrt{p^2 + q^2} \qquad (23)$$

respectively, where

$$a' = \tfrac{1}{2}(px_i + qy_i + r)$$

$$p = y_j - y_k$$

$$q = x_k - x_j$$

$$r = x_j y_k - x_k y_j \qquad (24)$$

and $i$, $j$ and $k$ are the vertices of the triangle. In this fashion, the height $h$ of a triangle after rezoning is given by

$$h = 2a/b. \qquad (25)$$

This characterizes the first term of (20).

We next consider the second term of eqn (20). If the generic triangle in Fig. 2 were isosceles, its vertex $P_i$ would be located at a point with coordinates

$$x_t = x_m + \frac{p}{b^2} 2a$$

$$y_t = y_m + \frac{q}{b^2} 2a, \qquad (26)$$

where

$$x_m = (x_j + x_k)/2$$

$$y_m = (y_j + y_k)/2, \qquad (27)$$

and distance $d$ would read

$$d = \sqrt{(x_i + l_x - x_t)^2 + (y_i + l_y - y_t)^2}. \qquad (28)$$

The mean basis of the triangles is (see eqn (23))

$$\bar{b} = \frac{\sum_{\acute{n}} b}{\acute{n}}. \qquad (29)$$

By using this formulation, $\hat{D}$ depends on $l_x$ and $l_y$. The optimal position for node $P_i$ is that which makes $\hat{D}$ a minimum,

$$\begin{cases} \dfrac{\partial \hat{D}}{\partial l_x} = 0 \\[2mm] \dfrac{\partial \hat{D}}{\partial l_y} = 0 \end{cases} \qquad (30)$$

which can be elaborated as

$$\begin{cases} s_1 l_x + s_2 l_y = s_3 \\ s_2 l_x + s_4 l_y = s_5 \end{cases}. \qquad (31)$$

Using Cramer's rule, an explicit solution can be obtained:

$$l_x = \frac{s_3 s_4 - s_2 s_5}{s_1 s_4 - s_2^2}$$

$$l_y = \frac{s_1 s_5 - s_2 s_3}{s_1 s_4 - s_2^2}, \qquad (32)$$
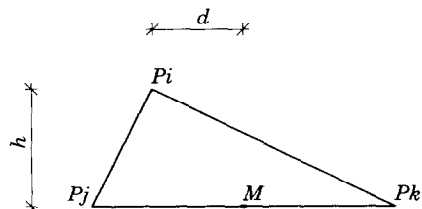


Fig. 2. Basic elements of a generic triangle.

wherein

$$s_1 = \sum_{\tilde{n}} \frac{1}{b^2} (w_1 p^2 + w_2 q^2)$$

$$s_2 = \sum_{\tilde{n}} \frac{pq}{b^2} (w_1 - w_2)$$

$$s_3 = \sum_{\tilde{n}} \frac{1}{b^2} (w_1 p(h^*b - 2a') - w_2 q((x_i - x_m)q$$

$$- (y_i - y_m)p)) \tag{33}$$

$$s_4 = \sum_{\tilde{n}} \frac{1}{b^2} (w_1 q^2 + w_2 p^2)$$

$$s_5 = \sum_{\tilde{n}} \frac{1}{b^2} (w_1 q(h^*b - 2a') - w_2 p((y_i - y_m)p$$

$$- (x_i - x_m)q)), $$

and

$$w_1 = t/h^{*2}$$

$$w_2 = 4(1 - t)/\bar{b}^2. \tag{34}$$

### 3.4. Iteration procedure

The mesh density should be evaluated at the centre of each element. This does not result in a fixed point upon rezoning of node $P_i$, and system (31) would become non-linear. Since system (31) must be linear, a fixed point as close as possible to the centre of the element must be found. Point $M$ (Fig. 2) is chosen for this purpose. The ideal area is computed as the inverse of the mesh density:

$$A = \frac{1}{\delta}, \tag{35}$$

which is obtained via a restriction of equation (8) to the influence domain $\Omega_i$,

$$\delta = \frac{\hat{n}w}{\int_{\Omega_i} w \, d\Omega}. \tag{36}$$

This restriction ensures that node $P_i$ will remain inside its influence domain after rezoning, because the calculated ideal area will be always smaller than the influence domain area. This is of pivotal importance for updating the weight function, as will be explained next. Once the ideal area $A$ is known, the height $h^*$ is obtained as

$$h^* = 2A/b. \tag{37}$$

The global configuration of the mesh cannot be obtained with the Gauß–Seidel procedure as has been used by [9], because the updating of the nodal density

values would induce a loss of symmetry in symmetrical domains. The adopted procedure is the Jacobi method. When computing the new position of node $P_i$ within iteration $k$, the new position of nodes $P_1-P_{i-1}$ is not considered. In other words, the rezoning of each node is computed on the resulting mesh from the previous iteration.

When an iteration is completed, the density function must be updated on the new nodal positions, so that the rezoning may be continued. A first step to do so is to find the element in which a node is now located, and to perform an interpolation by means of its shape functions. This procedure can be reasonable in rectangular domains with structured meshes, where the element to which a given nodal point belongs can be determined via the spatial coordinates of the nodal point. Otherwise, it is too expensive, because the searching of the current element results in a procedure which requires a number of operations proportional to the square of the number of elements.

The constraint that a node remains within its influence domain via eqn (36) limits the searching to the elements which surround it. First, the triangle to which the point, with coordinates $x$ and $y$, belongs is determined via evaluation of the quantities

$$\frac{1}{2} \begin{vmatrix} x_i & y_i & 1 \\ x_j & y_j & 1 \\ x & y & 1 \end{vmatrix} \quad \frac{1}{2} \begin{vmatrix} x_j & y_j & 1 \\ x_k & y_k & 1 \\ x & y & 1 \end{vmatrix} \quad \frac{1}{2} \begin{vmatrix} x_k & y_k & 1 \\ x_i & y_i & 1 \\ x & y & 1 \end{vmatrix}, \tag{38}$$

where $x(i,j,k)$, $y(i,j,k)$ are the coordinates of the vertices defined in Fig. 2. Quantities (38) account for the respective areas of the triangles defined by the point $(x, y)$ and every side of the currently evaluated triangle in the influence domain. The properties of determinants make these quantities simultaneously positive if, and only if, point $(x, y)$ is in the current triangle. In practice, a negative number close to zero (approximately $-10^{-9}$, depending on the machine precision) times the area of the current triangle is used as the tolerance, in order to overcome round-off errors. Any further loss of accuracy derived from this approximation has no importance in the context of a remeshing process. Once the element has been found, parameters $\xi$ and $\eta$ are computed through the inverse of the isoparametric transformation,

$$\xi = \frac{xc_1 - yc_2 + x_1 y_4 - x_4 y_1 + x_2 y_3 - x_3 y_2}{-xc_5 + yc_6 - x_1 y_4 + x_4 y_1 + x_2 y_3 - x_3 y_2}$$

$$\eta = \frac{xc_3 - yc_4 + x_1 y_2 - x_2 y_1 + x_4 y_3 - x_3 y_4}{-xc_5 + yc_6 - x_1 y_2 + x_2 y_1 + x_4 y_3 - x_3 y_4}, \tag{39}$$

where

$$c_1 = y_1 + y_2 - y_3 - y_4$$

$$c_2 = x_1 + x_2 - x_3 - x_4$$

$$c_3 = y_1 - y_2 - y_3 + y_4$$

$$c_4 = x_1 - x_2 - x_3 + x_4$$  (40)

$$c_5 = y_1 - y_2 + y_3 - y_4$$

$$c_6 = x_1 - x_2 + x_3 - x_4$$

and $x_n, y_n, n = 1$–$4$, are the coordinates of the nodal points. This inverse isoparametric transformation has not been found by inverting the direct isoparametric transformation, because it would have been tedious and complicated. It is obtained in a relatively simple manner by considering that point $(x_0, y_0)$, the anti-image of $(\xi_0, \eta_0)$, is on coordinate lines $\xi = \xi_0$ and $\eta = \eta_0$. Every coordinate line is linearly interpolated between the coordinate lines $\xi = 1$, $\xi = -1$ and $\eta = 1, \eta = -1$ respectively, which give the sides of the element in the physical space. Since the nodal coordinates in the physical space, $(x_n, y_n)$, $n = 1$–$4$ are known, the implicit equation of the element sides may be derived. The implicit equation of the coordinate lines may also be found, because these lines contain point $(x_0, y_0)$ and, respectively, the common point of the support line of each pair of opposed element sides. The values of $\xi_0$ and $\eta_0$ are then isolated by considering the coefficients of both implicit equations interpolated between the coefficients of the element sides.

Finally, the value of the weight function is obtained by means of interpolation with the shape functions,
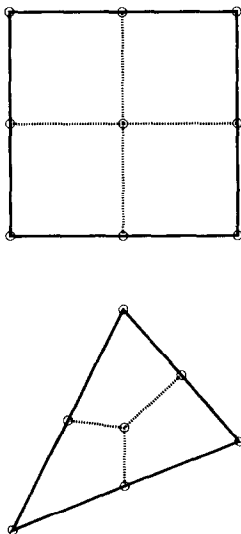


Fig. 3. Splitting of higher-order elements.
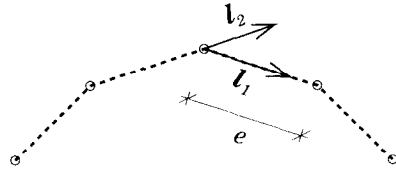


Fig. 4. Decomposition of the rezoning of a boundary node.

$$w(x, y) = w(x_1, y_1)N_1(\xi, \eta) + w(x_2, y_2)N_2(\xi, \eta)$$

$$+ w(x_3, y_3)N_3(\xi, \eta) + w(x_4, y_4)N_4(\xi, \eta). \quad (41)$$

### 3.5. *Rezoning of higher-order elements*

Rezoning of higher order elements requires that a background mesh of linear elements is supplied. When the process is completed, all the auxiliary constructions are erased and the original topology is recovered.

Nine-node elements can easily be split in four linear quadrilaterals. In a similar fashion, eight-node elements are split in four quadrilaterals by adding a central node (Fig. 3).

Six-node triangles can be split in four linear triangles. Nevertheless, the modified rezoning algorithm behaves in an unstable manner when linear triangles are used, because the point where the mesh density must be evaluated (the centre of the element) does not remain fixed after rezoning of every node and system (31) would be non-linear. For this reason it is preferable to split six-node triangles into three quadrilaterals by adding a central node (Fig. 3).

### 3.6. *Rezoning of a boundary node*

The nodal points which are on the boundary must remain on the boundary, but not necessarily at the same position. A possible approach to do so can be found in Huétink *et al.* [4], which consists of projecting the old nodal positions on a locally interpolated spline. However, in the case we are concerned with, the use of quadratic or higher order curves is not justified, since simpler methods can be used. The results obtained via a simple projection of the rezoned node on the boundary are generally unsatisfactory, even for straight contours. Below a constrained minimization of the influence domain, distortion will be used to achieve the rezoning of these nodes.

3.6.1. *Rezoning along a straight contour.* The presence of a prescribed translation direction may be taken as a constraint in the fashion

$$\alpha l_x + \beta l_y = 0, \quad (42)$$

where $(-\beta, \alpha)$ is the prescribed direction. Use of the Lagrange Multiplier method for minimizing the distortion as defined in (21) yields the system

$$\begin{cases} \dfrac{\partial \hat{D}}{\partial l_x} + \alpha\lambda = 0 \\[2mm] \dfrac{\partial \hat{D}}{\partial l_y} + \beta\lambda = 0 \\[2mm] \alpha l_x + \beta l_y = 0 \end{cases} \qquad (43)$$

with $\lambda$ the Lagrange multiplier. The solution of eqn (43) is given by

$$l_x = \alpha c$$

$$l_y = \beta c, \qquad (44)$$

where

$$c = \frac{(\alpha s_3 + \beta s_5)}{\alpha(\alpha s_1 + \beta s_2) + \beta(\alpha s_2 + \beta s_4)}. \qquad (45)$$

3.6.2. *Rezoning along a curved contour.* Rezoning of a node which must follow a curved boundary may occur along two directions $l_1$ and $l_2$ defined by the previous and the next node respectively (Fig. 4). Solution of system (43) yields a translation along each

direction. The true rezoning of the node should follow a smooth curve through the previous node, the current node and the following node. An example is a curve such that the node is moved along the bisectrix of directions $l_1$ and $l_2$, if it remains near its original position, but when it is moved further its direction should be closer to $l_1$. The rezoning $l$ can then be obtained as a weighted mean of $l_1$ and $l_2$:

$$l = \frac{1}{1+\gamma}(l_1 + l_2), \qquad (46)$$

where

$$\gamma = \left(1 - \frac{\|l_1\|}{e}\right) \qquad (47)$$

is a measure of the amount a node is moved and $e$ is the distance to the next node in direction $l_1$. This procedure results in a satisfactory description of the boundary. Only small distortions of the original contour have been observed in zones of high curvature and low density. These constraints are not only useful for rezoning at the boundaries, but also at material discontinuities.
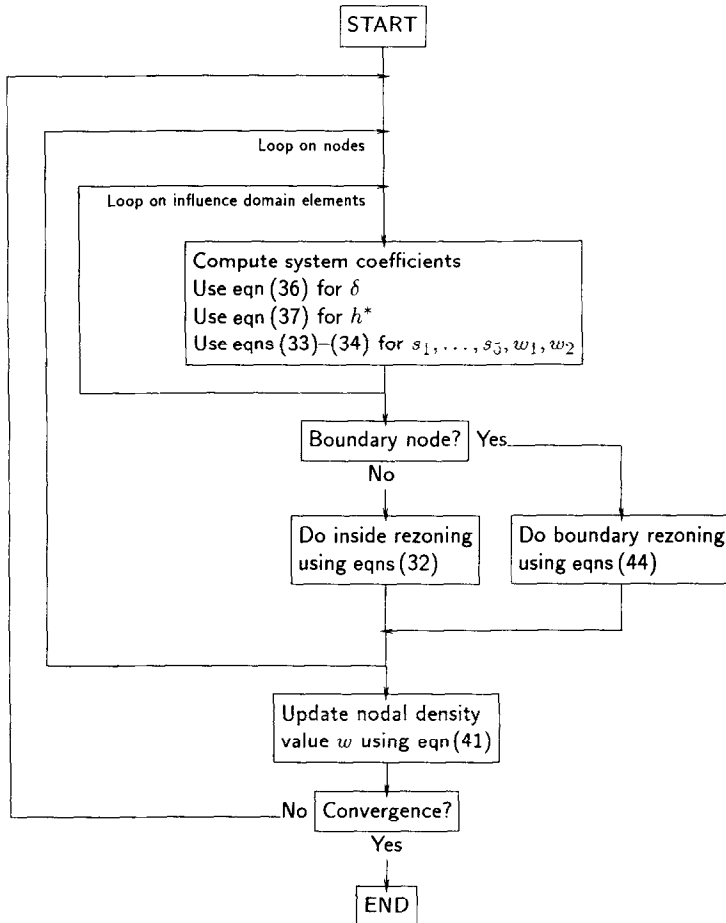


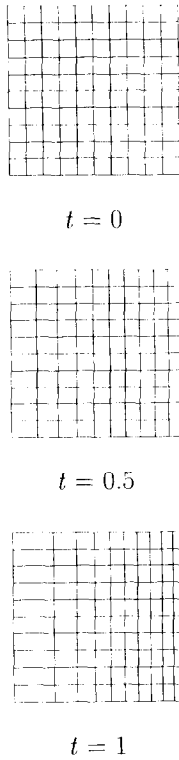Fig. 5. Flow chart of the developed algorithm.

$$t = 0$$



$$t = 0.5$$



$$t = 1$$

Fig. 6. Relative influence of the parameter $t$ on the results.

The organization of the algorithm is represented by the flow chart in Fig. 5.

### 3.7. *Examples*

In this section, some examples will be shown and the influence of parameter $t$ will be discussed. Figure 6 shows the resulting meshes for different values of $t$, for a regular mesh with a linear weight variation, ranging from 1 at the left edge to 10 at the right edge. On one hand, when $t = 0$, a completely regular mesh is obtained, and no refinement is observed. On the other hand, for $t = 1$ the size of each element is in accordance with the weight function at its centre. An intermediate situation is obtained for $t = 0.5$.

Figure 7 shows the remeshing of an L-shaped domain with a trilinear density function. The description of curved boundaries is illustrated in Fig. 8, for a linear weight variation from five (left) to one (right). A slight deviation from the original contour is observed at the right side, where the mesh density is lower.

### 4. APPLICATION TO STRAIN LOCALIZATION

The developed algorithm will be used to improve the solution of a biaxial shear band test. This test consists of a rectangular von Mises plane-strain softening material specimen, submitted to a vertical force. Cosserat's elasto-plasticity theory has been used to assure convergence to a finite shear band

width upon mesh refinement. In the two-dimensional Cosserat continuum, a rotational degree-of-freedom, $\omega_z$, is introduced in addition to the translational degrees-of-freedom $u_x$ and $u_y$. While the definition of the normal strains is as normal, the definition of the shear strains is now

$$\epsilon_{xy} = \frac{\partial u_y}{\partial x} - \omega_z$$

$$\epsilon_{yx} = \frac{\partial u_x}{\partial y} + \omega_z. \tag{48}$$

This gives a difference between the macro-rotation

$$\Omega_z = \frac{1}{2}\left(\frac{\partial u_y}{\partial x} - \frac{\partial u_x}{\partial y}\right) \tag{49}$$

and the micro or Cosserat rotation $\omega_z$ equal to

$$\Omega_z - \omega_z = \tfrac{1}{2}(\epsilon_{xy} - \epsilon_{yx}). \tag{50}$$

This skew-symmetric part of the strain tensor can be related to the skew-symmetric part of the stress tensor $\frac{1}{2}(\sigma_{xy} - \sigma_{yx})$, as follows
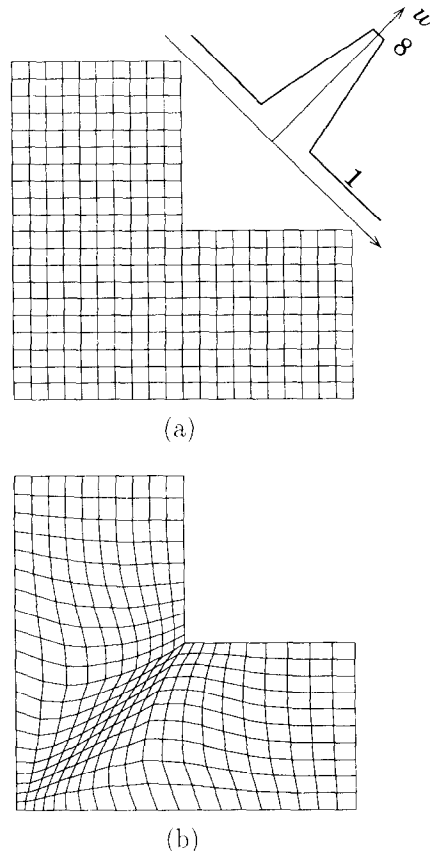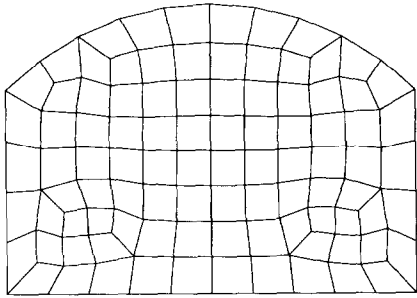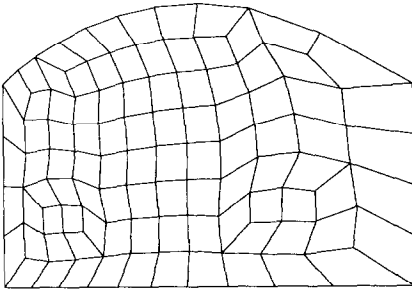


(a)



(b)

Fig. 7. Rezoning of an L-shaped domain; (a) original mesh, (b) resulting mesh.

(a)



(b)

Fig. 8. Example of a curved boundary; (a) original mesh, (b) resulting mesh.

$$\epsilon_{xy} - \epsilon_{yx} = 2\mu_c(\sigma_{xy} - \sigma_{yx}) \tag{51}$$

with $\mu_c$ an additional elastic parameter. The introduction of rotational degrees-of-freedom causes micro-curvatures, $\kappa_{xz}$ and $\kappa_{yz}$, to enter the set of strain components:

$$\kappa_{xz} = \frac{\partial\omega_z}{\partial x}$$

$$\kappa_{yz} = \frac{\partial\omega_z}{\partial y}. \tag{52}$$

They can be related to the conjugate stress components, the couple stresses $m_{xz}$ and $m_{yz}$, via

$$m_{xz} = 2\mu l^2 \kappa_{xz}$$

$$m_{yz} = 2\mu l^2 \kappa_{yz}, \tag{53}$$

with $l$ a fourth elastic constant, which has the dimension of length. A full treatment of the elasto-plastic Cosserat continuum, which is employed in the example, has been presented by de Borst [12].

The material properties have been taken as shear modulus $\mu = 4000$ N/mm² and Poisson ratio $v = 0.49$. The yield stress is $f_y = 100$ N/mm² and the softening modulus $h = -400$ N/mm². The two extra material parameters of the Cosserat continuum, $\mu_c$

and $l$, have been taken as $\mu_c = 2000$ N/mm² and $l = 2.5$ mm. The boundary conditions have been set such that the rotation $\omega_z$ is free on all sides (natural boundary conditions). The bottom of the sample is rigid and smooth ($u_y = 0$) and a vertical force, controlled by an arc-length method, is applied on the top of the sample.

### 4.1. Preliminary analysis

A preliminary analysis has been performed on a constant density 6 × 12-mesh where each quadrilateral consists of four, crossed, quadratic triangular elements. The conditions given above lead to a uniform distribution of the stress and an imperfection must be made in one element to trigger localization. In this case, it has been applied in the middle of the left edge of the specimen. Figure 9 shows the equivalent plastic strain ($\epsilon^p$) for approximately 80% post-peak residual force. The equivalent plastic strain is reproduced with a poor resolution, if we compare it with a reference solution obtained with a 12 × 24-mesh (Fig. 9). Below, we shall construct two improved 6 × 12-meshes. First, the amount of plastic strain is used as criterion for remeshing. Then, the difference between macro-rotation $\Omega_z$ and micro-rotation $\omega_z$ is used as an indicator to improve the mesh spacing locally.

### 4.2. Remeshing

The indicators discussed in the previous section cannot directly be used as weight function, because they are equal to zero in large parts of the domain. The relation between the sizes of the largest and the smallest elements must be introduced. For this purpose we shall follow Eiseman [5], who obtains the weight function $w$ as follows. Let $R$ be the refinement indicator assumed positive, e.g. $R = \epsilon^p$ or $R = |\Omega_z - \omega_z|$, in a domain $\Omega$; the weight function is then obtained as

$$w = r\frac{R}{\max_{\Omega}(R)} + s. \tag{54}$$

In this fashion, $w$ is bounded

$$s \leqslant w \leqslant r + s \tag{55}$$

and the constants $r$ and $s$ are chosen so that

$$\frac{r+s}{s} = \rho, \tag{56}$$

with $\rho$ the relation between the sizes of the largest and the smallest elements. In this case it has been chosen equal to five ($r = 4, s = 1$).

The appearance of both meshes is quite different for each criterion (Fig. 10). When the equivalent plastic strain is used, the mesh is densified, especially in the lower right corner, i.e. where the largest strains
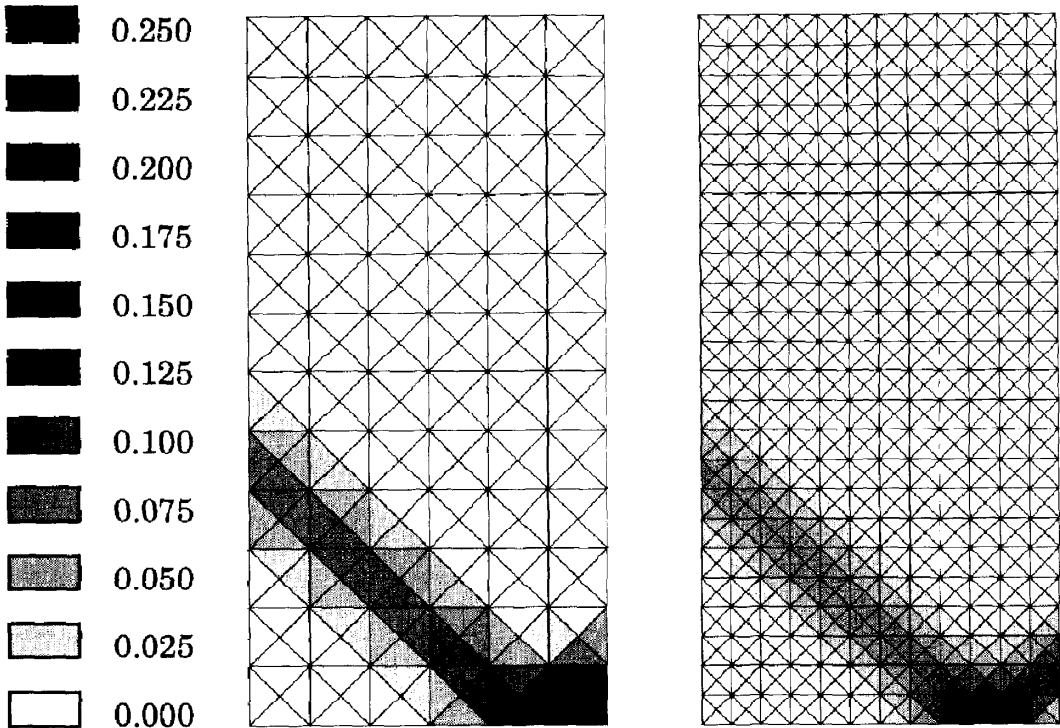
Fig. 9. Representation of the equivalent plastic strain for the biaxial analysis. Left: coarse mesh. Right: fine mesh.
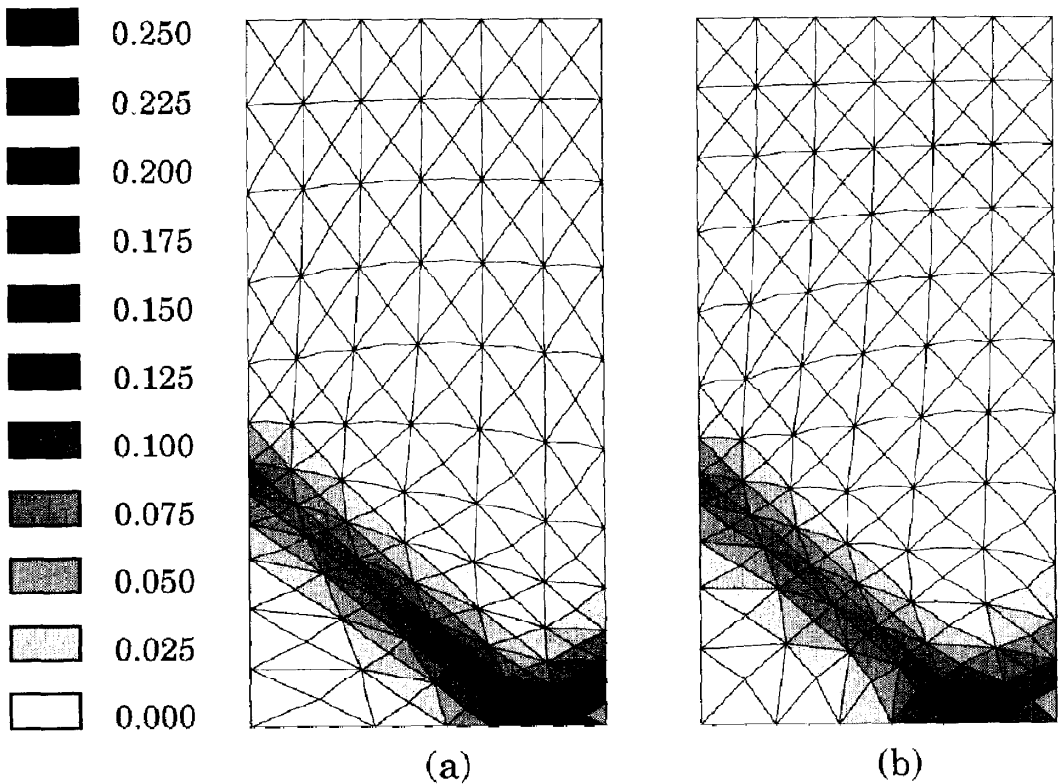


(a)                                                                    (b)

Fig. 10. Comparison of the results obtained with the adapted meshes according to both criteria; (a) equivalent plastic strain, (b) difference between macro and micro-rotation.

appear. In contrast, the difference between macro-rotation and micro-rotation yields a fine mesh along the shear band, but results in a somewhat coarser mesh in the lower right corner. This result is logical since compression, rather than shear, governs the local behaviour in this corner.

Finally, it is mentioned that the boundary nodes have been allowed to move along their respective edge but that the corner nodes have been kept fixed.

### 4.3. *Analysis with the adapted mesh*

The analysis has been repeated with the adapted meshes. The necessary imperfect zone cannot be kept on its original position, because all the elements have been moved. Instead it has been placed in the closest element to the imperfect zone in the original configuration. Figure 10 shows the obtained equivalent plastic strain for approximately 80% residual force. In both cases, the accuracy of the solution has been improved along the shear band. However, different results have been obtained on the lower right corner. The mesh which has been adapted using the equivalent plastic work criterion gives a good approximation of the reference solution. Conversely, when the difference between rotations is used as remeshing criterion, the solution is hardly improved in this area.

### 5. CONCLUDING REMARKS

An efficient algorithm has been developed for rezoning of the finite element mesh. The mesh is densified where needed, while the global topology is unchanged. Problems like the continued interpolation of the weight function and the description of curved boundaries have been successfully overcome.

Mesh adaptivity has been performed in a biaxial shear-band test for a von Mises strain softening Cosserat material. The equivalent plastic strain and the difference between macro–rotation and micro-rotation have been used as remeshing indicators. The results have been improved in both cases, while the computational cost remains constant.

### REFERENCES

1. L. J. Sluys, Wave propagation, localisation and dispersion in softening solids. Dissertation, Delft University of Technology, The Netherlands (1992).
2. J. Donea, Arbitrary Lagrangian-Eulerian finite element method. *Computer Methods in Mechanics: Volume 1, Computer Methods for Transient Analysis* (Edited by T. Belytschko and T. J. R. Hughes). North Holland, Amsterdam (1983).
3. A. Huerta, G. Pijaudier-Cabot and L. Bode, Mesh adaptivity in a transient finite element analysis with a nonlocal model. *Proc. of Fracture Mechanics of Concrete Structures I* (Edited by Z. P. Bažant), pp. 321–329. Elsevier, New York (1992).
4. J. Huétink, P. T. Vreede and J. van der Lugt, Progress in mixed Eulerian–Lagrangian finite element simulation of forming processes. *Int. J. Numer. Meth. Engng* **30**, 1441–1457 (1990).
5. P. R. Eiseman, Adaptive grid generation. *Comput. Meth. Appl. Mech. Engng* **64**, 321–376 (1987).
6. J. F. Thompson, Z. U. A. Warsi and C. W. Mastin, *Numerical Grid Generation: Foundations and Applications.* North Holland, Amsterdam (1985).
7. D. Catherall, The adaptation of structured grids to numerical solutions for transonic flow. *Int. J. Numer. Meth. Engng* **32**, 921–937 (1991).
8. D. Dinkler, B. Kröplin and G. Peffer, Conservation of topology in adaptive remeshing. *Proc. of the 3rd Int. Conf. on Numer. Grid Generation in Comp. Fluid Dyn. and Related Fields* (Edited by A. Sánchez-Arcilla, J. Hauser, P. R. Eiseman and J. F. Thompson). North Holland, Amsterdam (1991).
9. S. Giuliani, An algorithm for continuous rezoning of the hydrodynamic grid in arbitrary Lagrangian–Eulerian computer codes. *Nucl. Engng Des.* **72**, 205–212 (1982).
10. M. A. Gutiérrez, Utilization of adaptivity techniques in strain localization problems. Report 25.2.93-2.21, Delft University of Technology, The Netherlands (1993).
11. S. Cescotto and Z. D. Wu, A variable-density mesh generation for planar domains. *Commun. Appl. Numer. Meth.* **5**, 473–481 (1989).
12. R. de Borst, A generalization of $J_2$-flow theory for polar coninua. *Comput. Meth. Appl. Mech. Engng* **103**, 347–362 (1993).